Semiempirical van der Waals interactions versus *ab initio* nonlocal correlation effects in the thiophene-Cu(111) system

Martin Callsen, Nicolae Atodiresei,[*] Vasile Caciuc, and Stefan Blügel

Peter Grünberg Institut (PGI-1) and Institute for Advanced Simulation (IAS-1), Forschungszentrum Jülich and JARA, 52425 Jülich, Germany

The adsorption mechanism of single thiophene (C_4H_4S), 4-thiophene ($C_{16}H_{10}S_4$), and their dimers on the Cu(111) surface has been studied in the framework of the density functional theory (DFT). The importance of the London dispersion effects on the molecule-surface adsorption geometry and the corresponding binding energy was investigated by using semiempirical and first-principles methods. Interestingly, the physisorption character of the thiophene bonding on Cu(111) suggested by strength of the molecule-surface interaction as revealed by the DFT calculations turns out to be a weak chemisorption even for the DFT ground-state geometry when a nonlocal correlation energy functional [Dion *et al.*, Phys. Rev. Lett. **92**, 246401 (2004)] is used. Our *ab initio* calculations also suggest that the formation of thiophene and 4-thiophene dimers is energetically favorable with respect to the adsorption of single molecules.

I. INTRODUCTION

The use of single molecules as basic functional units in molecular electronic devices represents an appealing route to overcome the intrinsic limits of the silicon-based technology used to manufacture integrated circuits.[1] In this respect, the viability of the theoretical concept[2] to integrate organic molecules in electronic devices was experimentally demonstrated for diodes,[3,4] field-effect transistors,[5] switches,[6,7] or ultrahigh-density memory circuits.[8]

A fundamental issue in molecular electronics is the ability to theoretically understand and thus to predict the properties of molecule-surface systems used in nanoelectronic devices. Of particular interest is the nature of the adsorbate-substrate interaction since its strength is one factor which controls the electron flow in a molecular-based device.[9,10] Among the molecule-surface systems of interest from this perspective, the thiophene (C_4H_4S) on a metal surface such as Cu(111) is an appealing choice since thiophene is a basic functional unit of oligothiophene used to build, for instance, a molecular field effect transistor[11] or molecular wires on the NaCl/Cu(111) system.[12]

From the experimental point of view, thiophene molecules adsorbed on the Cu(111) surface have been investigated by Milligan *et al.*,[13,14] Imanishi *et al.*,[15] and Rousseau *et al.*[16] In these normal incidence x-ray standing wave (NIXSW), near edge x-ray absorption fine structure (NEXAFS), and temperature programmed desorption (TPD) measurements, the focus was on the details of the ground-state geometry such as the adsorption site, the molecule-surface distance, and the tilt angle of the thiophene molecules for different coverages as well as on the corresponding adsorption energy. While no clear picture on the adsorption geometry of a single thiophene molecule on Cu(111) emerged from the experimental side, the TPD experiments suggest that a single thiophene is weakly chemisorbed on this substrate.

Besides this, the adsorption of single or a self-assembled monolayer (SAM) of oligothiophene molecules with a different molecular length on several metal surfaces was also studied. For instance, the 6-thiophene ($C_{24}H_{14}S_6$) on Cu(110)

was experimentally investigated by Kiguchi *et al.*[17] Recently, Kakudate *et al.*[18] have examined the adsorption of 8-thiophene ($C_{32}H_{20}S_8$) on the Cu(111) surface at room temperature. Their study revealed that on this substrate, these molecules form a chainlike structure whose orientation depends on the coverage. More specifically, at low coverages the molecular chains are oriented along the ⟨11-2⟩ surface direction while with increasing coverage the 8-thiophene chains start to align along the ⟨110⟩ direction too.

From the theoretical point of view, a single thiophene adsorbed on metal surfaces such as Ni(100),[19] Ni(110),[20] Pd(100),[19] Cu(100),[19] Cu(110)[21], Cu(111),[22] and Au(111)[22–24] has been investigated by means of the density functional theory (DFT). These studies indicate that thiophene interacts strongly with the Ni(110) and Ni(100) substrates leading to its desulfurization while this process does not occur in the case of the Pd(100), Cu(100), Cu(110), Au(111), and Cu(111) surfaces. Importantly, as discussed in detail in Refs. 21 and 22, the proper description of a single thiophene molecule adsorbed on the Cu(110) and Cu(111) surfaces required the inclusion of the van der Waals (vdW) interactions in their DFT calculations.

In this theoretical study we have focused on the investigation of the structural and electronic properties of single thiophene (C_4H_4S) as well as 4-thiophene ($C_{16}H_{10}S_4$) and their dimers on the Cu(111) surface. In the case of a single thiophene on Cu(111), the London dispersion effects whose importance was emphasized in Refs. 21 and 22 are described by using two semiempirical approaches and a first-principles approach. In particular, the use of an *ab initio* exchange-correlation functional designed to include the nonlocal correlation effects responsible for the vdW interactions allowed us a unique insight into the importance of the nonlocal vs semilocal contribution to the adsorption energy of this system. More specifically, although the charge transfer at the molecule-surface interface indicates the formation of a chemical bond, the DFT calculations predict that the strength of the interaction between a single thiophene molecule and the Cu(111) surface would correspond rather to a physisorption. However, the use of the nonlocal correlations instead of the semilocal

ones for the DFT relaxed geometry corrects this strength to that expected for a weak chemisorption. Furthermore, the relevance of the London dispersion effects on the molecule-surface adsorption geometry and its binding energy for a single 4-thiophene and dimers of thiophene and 4-thiophene molecules have also been investigated. The DFT calculations and those including the vdW interactions suggest that the thiophene and 4-thiophene dimers are energetically more favorable with respect to the adsorption of single molecules.

II. COMPUTATIONAL METHOD

Our *ab initio* calculations have been carried out in the framework of DFT as implemented in the VASP code.[25–28] As approximation for the exchange correlation functional we applied the generalized gradient approximation (GGA) in the parametrization of Perdew, Burke, and Ernzerhof (PBE).[29] The projector augmented wave (PAW) method developed by Blöchl[30] has been used. The wave functions are expanded in a plane wave basis up to a cutoff energy of 500 eV. For structural relaxations only the Γ point was used to sample the Brillouin zone.

The Cu(111) surface has been modeled by a six-layer slab separated from its periodically repeated image by 15 Å of vacuum, using the theoretical lattice constant for Cu of 3.63 Å. The upper three layers and the adsorbed molecule were fully relaxed until forces became smaller than 0.003 eV/Å. For the single thiophene molecule (C_4H_4S) we used a $5 \times 3\sqrt{3}$ unit cell while the thiophene dimers were calculated in a $6 \times 4\sqrt{3}$, the single 4-thiophene molecule ($C_{16}H_{10}S_4$) in a $9 \times 3\sqrt{3}$, and the 4-thiophene dimer in a $14 \times 4\sqrt{3}$ unit cell. Due to computational costs, the number of layers was reduced for the latter to only three layers with the uppermost one allowed to relax.

The strength of the molecule-surface interaction can be determined by evaluating the adsorption energy E_{ads} which is defined as the difference between the total energy of the relaxed molecule-metal system E_{tot} and the sum of the total energies of the clean surface $E_{\mathrm{Cu(111)}}$ and gas-phase molecule E_{mol}:

$$E_{\mathrm{ads}} = E_{\mathrm{tot}} - (E_{\mathrm{Cu(111)}} + E_{\mathrm{mol}}). \quad (1)$$

As already discussed in the literature,[31] the nonlocal correlation effects responsible for the dispersion interaction are not correctly treated by common local and semilocal approximations to the exchange-correlation energy functional such as the local density approximation (LDA) or generalized gradient approximation (GGA). In particular, Tonigold *et al.*[22] showed that a proper description of the thiophene-Cu(111) system requires the inclusion of long-range vdW interactions. Several attempts have been made to correct for this drawback and the solution is to either calculate the dispersion energy E_{disp} by semiempirical approaches or by applying recently developed *ab initio* nonlocal exchange-correlation functionals. The first class of methods calculates the dispersion energy of the system as a sum of two-particle interactions following the London's dispersion $-C_6/R^6$ law:[32]

$$E^{\mathrm{disp}} = -s_6 \sum_{A<B} f_{\mathrm{damp}}\left(R_A^{\mathrm{vdW}}, R_B^{\mathrm{vdW}}, R_{AB}\right) C_{6,AB}\, R_{AB}^{-6}. \quad (2)$$

In this study we used the scaling parameter s_6, damping function $f_{\mathrm{damp}}(R_A^{\mathrm{vdW}}, R_B^{\mathrm{vdW}}, R_{AB})$, vdW radii R_A^{vdW}, and C_6 coefficients $C_{6,AB}$ for the AB atomic pair as proposed by Grimme[33] and refer to it as DFT-D2 approach. Under the assumption that the total energy of the physical system can be strictly divided into DFT- and vdW-like contributions, E^{disp} will be added to the total energy of the DFT calculation to obtain the total energy as

$$E^{\mathrm{DFT\text{-}D2}} = E^{\mathrm{DFT}} + E^{\mathrm{disp}}. \quad (3)$$

It is important to note that this method has been already used to describe the adsorption of several organic molecules on metal surfaces.[34–37] In particular, the DFT-D2 approach leads to a reasonable molecule-surface equilibrium distance for flat π molecular systems[35,36] while the adsorption energy is usually overestimated due to the missing screening of the van der Waals interactions (see Sec. III B).

Recently, Grimme proposed a new semiempirical approach (DFT-D3)[38] which takes into account the chemical environment of the atoms by adding a dependency of the C_6 coefficients on fractional coordination numbers. For both methods, the forces acting on atoms due to vdW interactions can be calculated analytically and used to relax the geometry of the physical system of interest. We have implemented both DFT-D2 and DFT-D3 methods in a local version of VASP and used them to investigate the role of the long-range van der Waals interactions on the adsorption of thiophene on the Cu(111) surface.

One of the most widely used first-principles nonlocal correlation functionals is the vdW-DF developed by Dion *et al.*[39] In this case, the GGA correlation contribution E_c^{PBE} to the total DFT energy E^{DFT} is replaced by a local LDA contribution E_c^{LDA} and a nonlocal correlation part E_c^{NL} such that the total energy is given by the following expression:

$$E^{\mathrm{vdW\text{-}DF}} = E^{\mathrm{DFT}} - E_c^{\mathrm{PBE}} + E_c^{\mathrm{LDA}} + E_c^{\mathrm{NL}}, \quad (4)$$

where the nonlocal correlation energy E_c^{NL} is given by an integral over the charge density $n(\mathbf{r})$ and a kernel function $\phi(\mathbf{r}, \mathbf{r}')$ (see Ref. 39 for more details):

$$E_c^{\mathrm{NL}} = \frac{1}{2} \iint n(\mathbf{r})\, \phi(\mathbf{r}, \mathbf{r}')\, n(\mathbf{r}')\, d^3\mathbf{r}\, d^3\mathbf{r}'. \quad (5)$$

Recently, a very efficient scheme developed by Román-Pérez and Soler[40] to calculate the nonlocal correlation energy in the reciprocal space has been reported, which we have also implemented (see the Appendix) in our original real-space postprocessing code JuNoLo.[41]

To get a deeper understanding of the role played by the nonlocal correlation effects responsible for the vdW interactions in our system, we will use later the concept of the nonlocal correlation energy density e_c^{NL} which is defined by rewriting Eq. (5) as

$$E_c^{\mathrm{NL}} = \int e_c^{\mathrm{NL}}(\mathbf{r})\, d^3\mathbf{r}. \quad (6)$$
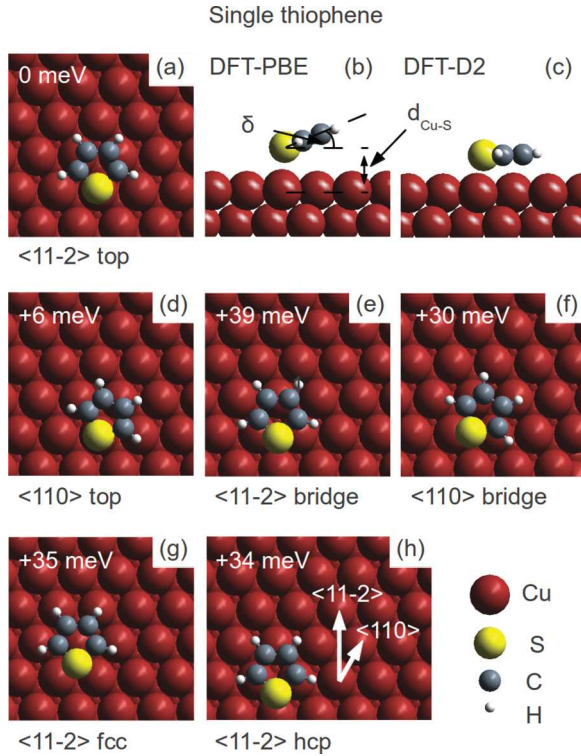
Single thiophene

FIG. 1. (Color online) The most stable configuration of a single thiophene molecule adsorbed on Cu(111) (upper panel). The side views (b) and (c) show the geometry obtained by DFT-PBE and DFT-D2 calculations. The tilt angle δ and the distance between molecule and surface $d_{\text{Cu-S}}$ defined in (b) are reduced when including the vdW corrections. (d)–(h) Some additional starting adsorption geometries are also shown. The energies specified for each adsorption configuration are the energy differences with respect to the DFT-PBE ground state which was set for convenience to 0 meV.

III. RESULTS

A. Adsorption geometry

As possible adsorption sites for a single thiophene molecule we calculated configurations with the sulfur atom occupying the top position of the Cu(111) surface [Fig. 1(a)], the bridge site [Fig. 1(e)], and the fcc [Fig. 1(g)] or hcp hollow [Fig. 1(h)] sites, which are the positions of high symmetry of the (111) surface. As a starting orientation, the molecule was oriented in the ⟨110⟩ and in the ⟨11-2⟩ direction of the surface or perpendicular to the surface. We also tried one orientation rotated by 15° with respect to the ⟨11-2⟩ direction but this configuration was not stable and rotated back to the ⟨11-2⟩ direction. As depicted in Fig. 1(a), within DFT-PBE the most stable adsorption geometry is with the S atom almost on top of a Cu one while the molecule is oriented in the ⟨11-2⟩ direction. The position of the S atom in the relaxed geometry is shifted away from the exact on top position by 0.18 Å in ⟨11-2⟩ direction. The distance between the S atom and the Cu atom directly underneath is 2.67 Å. Molecule-surface distances for the DFT-PBE, DFT-D2, and DFT-D3 methods are listed in Table I. In this configuration two of the three C-C bonds are positioned on top of a Cu atom. A change of the orientation to the ⟨110⟩ direction [see Fig. 1(d)] leads to an energy difference of 6 meV which is rather small. The configuration depicted

in Fig. 1(e) after moving the S atom from the top to the bridge position while keeping the orientation of the molecule fixed is 39 meV higher in energy. Thus for the adsorption of single thiophene molecules on the Cu(111) surface it is more important where the S atom is located than how the molecule is oriented.

Next we will shortly discuss the relaxation of the surface as the adsorption of sulfur-containing species on Cu(111) can lead to distortions of the surface. In the case of the adsorption of single S atoms it has been reported[42] that the strong interaction of S with the substrate leads to a significant, coverage-dependent distortion of the Cu(111) surface up to 0.1 Å displacement of nearest-neighbor atoms for the lowest coverage. In our case the distances to nearest-neighbor Cu atoms in the topmost surface layer is changed by less than 0.03 Å upon adsorption of thiophene. The Cu atom directly underneath the S atom is pulled out of the surface plane by 0.1 Å.

In Fig. 1(b) the side view of the thiophene molecule adsorbed on Cu(111) shows that the molecule is not adsorbed flat but tilted with respect to the plane of the surface by an angle $\delta = 18°$ without inclusion of vdW corrections. When we relax the system including vdW corrections via DFT-D2, only the configuration with S in the top position oriented in the ⟨11-2⟩ direction remains as a stable configuration while all other starting adsorption geometries relax towards this configuration. The distance between molecule and surface is reduced to 2.41 Å and the tilt angle vanishes. Using DFT-D3 gives a molecule surface distance of 2.66 Å which is almost the same as without correcting for vdW. The tilt angle of $\delta = 9°$ lies in between the DFT-PBE and the DFT-D2 result.

As already mentioned in the Introduction, experiments to determine the adsorption site, molecule surface distance, and tilt angle for thiophene adsorbed on Cu(111) by means of NEXAFS or NIXSW have been done by Imanishi *et al.*,[15] Milligan *et al.*,[13,14] and Rousseau *et al.*[16] In their extensive study on different coverages of thiophene on Cu(111), Milligan *et al.*[14] concluded that the thiophene molecule occupies a top position and is tilted by an angle of 26° ± 5° on the ideal Cu(111) surface for a 0.03 ML coverage with a distance between Cu and S of 2.62 ± 0.03 Å. In their work, the definition of 1 ML was one thiophene molecule per surface atom. Within this definition our coverage corresponds to 0.033 ML which is comparable to the experiment. When comparing the equilibrium molecule-surface geometries obtained with DFT-PBE, DFT-D2, and DFT-D3 approaches one can observe that for the DFT-PBE and DFT-D3 methods the adsorption position and the molecule-surface distance agree well with experiment. On the other hand, the DFT-D2 approach predicts a slightly too short molecule surface distance and, more importantly, the molecular plane lies almost flat on the Cu(111) surface at variance with experiment. As a preliminary conclusion, for a single thiophene on this copper metal surface, our *ab initio* calculations suggest that the DFT-D3 method provides a better description of its geometrical structure than the DFT-D2 one.

In addition to a single thiophene adsorbed on Cu(111), we have investigated three other systems, namely a thiophene dimer, a 4-thiophene ($C_{16}H_{10}S_4$), and its dimer on the same substrate in the limit of the DFT-PBE and DFT-D2 methods only. As will be discussed in more detail in Sec. III B, the reason for using DFT-D2 and not DFT-D3 is that DFT-D2

TABLE I. Adsorption energies E_{ads} in eV, the molecule-surface distances d_{Cu-S} in Å, and the tilt angle δ of single thiophene adsorbed on Cu(111) evaluated with the DFT-PBE, DFT-D2, and DFT-D3 methods. The vdW-DF values for the adsorption energy E_{ads} are obtained by postprocessing using the DFT-PBE, DFT-D2, and DFT-D3 relaxed geometries. It is important to note that in the case of the DFT-PBE relaxed geometry, the use of the vdW-DF functional modifies the strength of thiophene–Cu(111) surface interaction from that expected for physisorption to one characteristic to a weak chemisorption. On the other hand, the DFT-D2 approach significantly overestimates the experimental binding energy while the DFT-D3 calculations lead to a value remarkably close to it.

Geometry		DFT-PBE		DFT-D2		DFT-D3	
Method	Exp.[14]	DFT-PBE	vdW-DF	DFT-D2	vdW-DF	DFT-D3	vdW-DF
E_{ads} (eV)	−0.590	−0.137	−0.722	−1.018	−0.373	−0.605	−0.575
d_{Cu-S} (Å)	2.62 ± 0.03	2.67		2.41		2.66	
δ (°)	26 ± 5	18		0		9	

significantly overbinds compared to DFT-D3 which is critical to evaluate the reliability of our predicted adsorption geometry for 4-thiophene when compared with that suggested by STM experiments. Besides this, the DFT-D3 geometry is almost the same as the DFT-PBE one for the single thiophene molecule and only the value of the adsorption energy was modified by DFT-D3 calculations.

When we included a second thiophene molecule on the Cu(111) surface in order to form a dimer, both molecules adsorb with the S atoms on top of the Cu ones. In most of the configurations shown in Fig. 2 both molecules are oriented in the ⟨11-2⟩ direction. The tilt angle is the same as for a single thiophene molecule. The distance between the S atoms of two molecules and the corresponding surface Cu ones in the most stable configuration [see Fig. 2(a)] is 2.58 Å without vdW corrections and 2.40 Å with DFT-D2, being slightly shorter than that for a single thiophene molecule. Similarly to the single thiophene molecule, the calculated energy differences between the starting adsorption configurations are rather small.
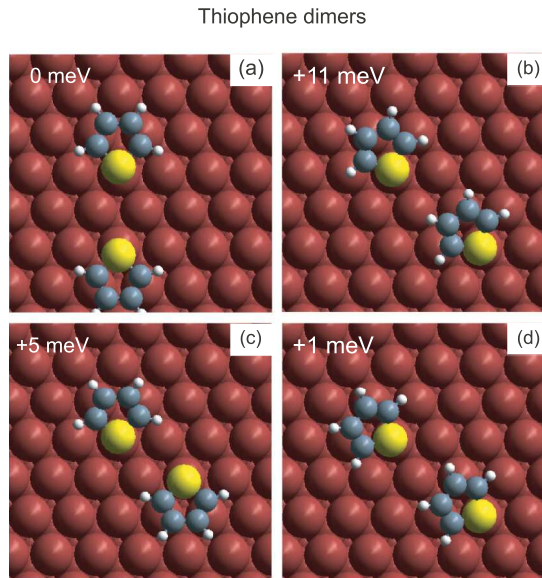
Thiophene dimers

FIG. 2. (Color online) The calculated adsorption geometries for dimers of single thiophene molecule among which (a) is the most stable configuration. The energies specified for each dimer adsorption geometry are the energy differences with respect to the DFT-PBE ground state which was set for convenience to 0 meV.

More specifically, in the case of the DFT-PBE calculations all configurations depicted in Fig. 2 are within a 11 meV energy range which suggest that several different dimer configurations can be experimentally observed. However, the energy difference between the most stable [see Fig. 2(a)] and the least stable configuration [see Fig. 2(b)] is increased to 103 meV when including vdW.

A recent STM study at room temperature showed that 8-thiophene molecules adsorb in chainlike structures on the Cu(111) surface.[18] This study suggests that the molecular chains are oriented in the ⟨11-2⟩ direction for low coverages. When the coverage was increased, molecular chains oriented in ⟨110⟩ direction were also observed. We studied the adsorption of the shorter 4-thiophene which is already a computationally demanding task. As for the single thiophene molecules the S atoms of the 4-thiophene molecule prefer to adsorb on top of Cu atoms. Due to the geometry of the Cu(111) surface the positions of the S atoms match perfectly with the positions of Cu atoms when the molecule is oriented in the ⟨110⟩ direction. This observation agrees well with the result of our first-principles calculations. The configuration of a 4-thiophene molecule adsorbed on Cu(111) oriented in the ⟨110⟩ direction [see Fig. 3(a)] is 58 meV lower in energy then that with the molecule oriented in the ⟨11-2⟩ direction. When we include the vdW corrections via the DFT-D2 approach, the difference is increased to 251 meV. Therefore, we obtain the opposite favored direction as observed in experiment for the cases of both DFT-PBE and DFT-D2 calculations. This conclusion is not changed when using the vdW-DF method for the DFT-PBE relaxed geometries since the molecular configuration along the ⟨110⟩ direction is 107 meV more stable than that along ⟨11-2⟩. Furthermore, we have also investigated a configuration with the molecule's short axis perpendicular to the surface but this configuration was not stable; i.e., it relaxed to the flat-lying adsorption configuration.

The relaxed geometry of the adsorbed 4-thiophene molecule is slightly bent. The outer two thiophene units have a distance between the S atoms and the underlying Cu atoms of 3.02 Å while the central two thiophene units have a larger distance of 3.18 Å without vdW corrections. Therefore, the average distance between the 4-thiophene molecule and the Cu(111) surface (3.10 Å) is thus significantly larger than that for a single thiophene molecule (2.67 Å). When applying DFT-D2 the molecule gets closer to the Cu(111) surface. The outer two thiophene units are 2.42 Å away from their
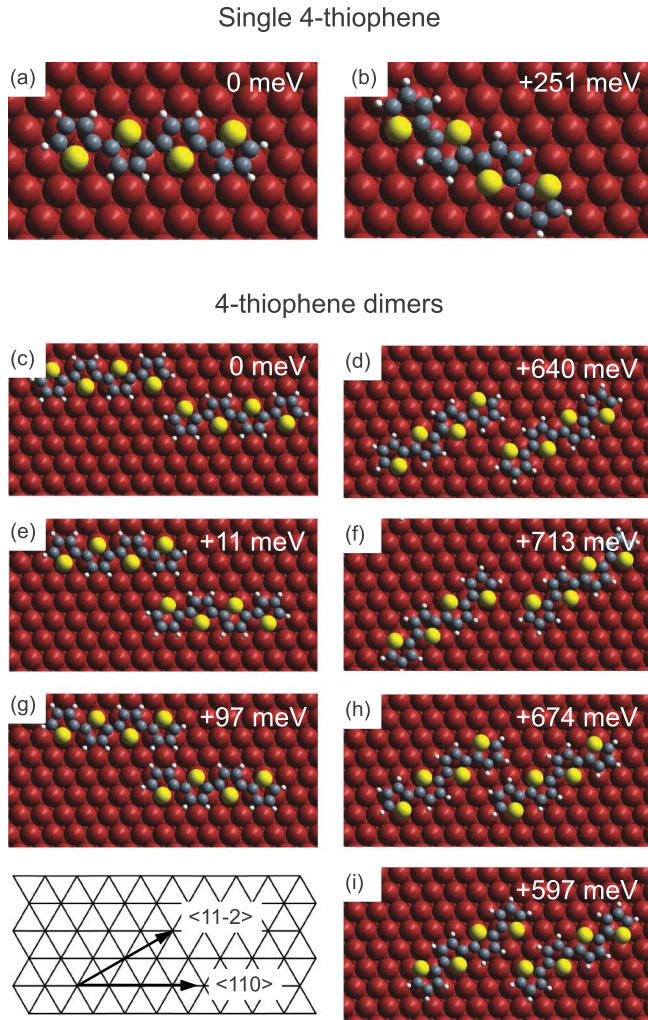
Single 4-thiophene

4-thiophene dimers

FIG. 3. (Color online) (a)–(b) 4-thiophene adsorbed on Cu(111) with the molecular long axis oriented along the $\langle 110 \rangle$ and $\langle 11\text{-}2 \rangle$ surface directions. Due to a better match between the molecule and the surface, the configuration (a) is more stable because more S atoms lie directly on top of the Cu ones. (c)–(i) The calculated adsorption configurations of 4-thiophene dimers on Cu(111) oriented along the $\langle 110 \rangle$ and $\langle 11\text{-}2 \rangle$ surface directions. Consistent with the DFT-D2 calculations for single 4-thiophene molecules on the Cu(111) surface, the 4-thiophene dimers prefer to adsorb with the molecular long axis oriented along the $\langle 110 \rangle$ direction. Among the shown configurations, the (c) geometry is the most stable one.

corresponding Cu atoms and the central two 2.49 Å. With vdW corrections the relaxed 4-thiophene molecule becomes less bent. Also in this case one can observe that DFT-D2 leads to a stronger change of the molecule surface distance for 4-thiophene than for single thiophene molecules.

The adsorption of a second 4-thiophene molecule on the Cu(111) surface conserves the preference for the adsorption along the $\langle 110 \rangle$ direction. Once again, the perfect match between the position of the S atoms of the 4-thiophene molecule oriented in the $\langle 110 \rangle$ direction and the Cu(111) surface leads to a stronger bonding of the molecules to the surface than for the dimers oriented along the $\langle 11\text{-}2 \rangle$ direction. Among all the calculated configurations, the least stable one oriented along the $\langle 110 \rangle$ direction [see Fig. 3(g)] is 500 meV

lower in energy than the most stable dimer oriented along the $\langle 11\text{-}2 \rangle$ direction [see Fig. 3(i)].

Kakudate *et al.*[18] observed in their STM experiment that the distance between two bright lobes of an 8-thiophene molecule is 4.4 Å and by this roughly 14% larger than the distance of 3.9 Å between two single thiophene units in the gas phase. As a possible explanation they proposed that the molecule is elongated when it adsorbs on the Cu(111) surface. In this case also the match between the molecule and the surface would favor the $\langle 11\text{-}2 \rangle$ direction as 4.4 Å is the distance to the next neighboring Cu atom along the $\langle 11\text{-}2 \rangle$ direction and each S atom would be able to adsorb on top of a Cu atom. To check the validity of this scenario, we performed calculations with a dimer of elongated 4-thiophene molecules adsorbed on the Cu(111) surface. When we allow the elongated 4-thiophene molecules to freely relax, they immediately return to their initial unstretched adsorption configuration as shown in Fig. 3(d). This behavior is due to the huge amount of energy required to elongate the intramolecular bonds. Similar calculations carried out with the S atoms kept fixed on top of the Cu ones lead to an elongated configuration which is 5.56 eV higher in energy. In consequence, our first-principles calculations clearly indicate that such elongated configurations are not energetically stable and further theoretical and experimental investigations are required to identify the origin of the disagreement between the STM experiments and our *ab intio* simulations.

B. Bonding mechanism

The adsorption energy of single thiophene molecules on the Cu(111) surface has been experimentally measured.[14] Its value $E_{\text{ads}}^{\text{exp}} = -590$ meV suggests that single thiophene molecules are weakly chemisorbed on the Cu(111) surface. For the DFT-PBE relaxed geometry of thiophene adsorbed on Cu(111) we obtain an adsorption energy of $E_{\text{ads}}^{\text{DFT-PBE}} = -137$ meV (see Table I) where the negative sign means that the molecule is bound to the surface. In a previous study, Tonigold *et al.*[22] obtained a smaller value of -0.070 meV which can be assigned to a higher coverage considered in their work. By comparing our calculated value (-137 meV) to the experimental one (-590 meV), one can observe that the theoretical adsorption energy is underestimated in DFT-PBE. However, when the adsorption energy for the relaxed DFT-PBE geometry was evaluated with the vdW-DF method, the obtained value $E_{\text{ads}}^{\text{vdW-DF}} = -722$ meV was significantly lower than its DFT-PBE counterpart and closer to the experimental one.

We have also calculated the single thiophene-Cu(111) adsorption energy for the relaxed geometries obtained with the DFT-D2 and DFT-D3 approaches. Including the vdW corrections via the DFT-D2 method leads to an adsorption energy of $E_{\text{ads}}^{\text{DFT-D2}} = -1018$ meV. One can observe that the DFT-D2 approach leads to a strong bonding between the molecule and the surface which overestimates the experimental value of the adsorption energy. This is due to the fact that within DFT-D2 all Cu atoms are treated with the same C_6 coefficient while in reality the polarizability and thus the corresponding C_6 coefficient should decrease with the increasing distance between the molecule's atoms and the Cu ones due to screening effects. As proposed in Ref. 37, a way to achieve a similar effect

TABLE II. Adsorption energies E_{ads} in eV given per molecule for the most stable DFT-PBE and DFT-D2 configurations of thiophene dimers, 4-thiophene, and 4-thiophene dimers adsorbed on Cu(111).

Molecule	Configuration	E_{ads} (eV/molecule)	
		DFT-PBE	DFT-D2
thiophene	Fig. 1(a)	−0.137	−1.018
thiophene dimer	Fig. 2(a)	−0.148	−1.112
4-thiophene	Fig. 3(a)	−0.344	−3.554
4-thiophene dimer	Fig. 3(c)	−0.392	−3.636

is to reduce the number of substrate layers which are taken into account when calculating the vdW corrections. When we apply this scheme to our system such that only the uppermost surface layer is interacting with the molecule, we obtain an adsorption energy of −806 meV. This value is closer to the experimental one than those obtained with DFT-PBE and DFT-D2. On the other hand, the self-consistent calculations with the DFT-D3 method gave an adsorption energy of $E_{ads}^{DFT-D3} = -605$ meV which is in remarkably good agreement with the experimental value. This surprisingly good agreement can be attributed to the fact that, in contrast to DFT-D2, in DFT-D3 the C_6 coefficients are distance and coordination number dependent and therefore the screening effect of the surface missing in DFT-D2 is partially mimicked.

The adsorption energies for thiophene dimers, 4-thiophene, and 4-thiophene dimers evaluated with the DFT-PBE and DFT-D2 approaches have been gathered in Table II. The adsorption energy of a single thiophene dimer per molecule is −148 meV without vdW and −1.112 eV employing DFT-D2. In both cases the adsorption energy is lower than the corresponding value for the single thiophene molecule which means that the formation of dimers is favored.

However, it is important to note that the DFT-PBE calculations predict that a single 4-thiophene molecule will adsorb along the $\langle 110 \rangle$ surface direction ($E_{ads}^{DFT-PBE} = -0.344$ eV) at variance with the experimental STM results[18] which suggest that it lies along the $\langle 11\text{-}2 \rangle$ direction ($E_{ads}^{DFT-PBE} = -0.286$ eV). Similarly, the DFT-PBE adsorption energies for the 4-thiophene dimer configurations shown in Figs. 3(d) and 3(i) (along the $\langle 11\text{-}2 \rangle$ direction) are by 153 and 115 meV higher than that presented in Fig. 3(c) (along the $\langle 110 \rangle$ surface direction). These observations led us to use also the DFT-D2 method for these systems as a limiting theoretical case since we have already shown that, in comparison with the DFT and DFT-D3 approaches, for a single thiophene molecule on Cu(111) the DFT-D2 calculations significantly overestimate the adsorption energy and distort its geometry more than the experiments[14] suggest. Then, for a single 4-thiophene molecule we obtain an adsorption energy of −0.344 eV without vdW and −3.554 eV when applying DFT-D2. Note that the DFT-D2 approach predicts the same ground state as the DFT-PBE one with the 4-thiophene molecule aligned along the $\langle 110 \rangle$ direction still in disagreement with experiment. Nevertheless, both DFT-PBE and DFT-D2 calculations indicate that the 4-thiophene molecule is bound stronger to the Cu(111) substrate than a single thiophene molecule. Besides this, the adsorption energy per molecule for the 4-thiophene dimer suggests that also in
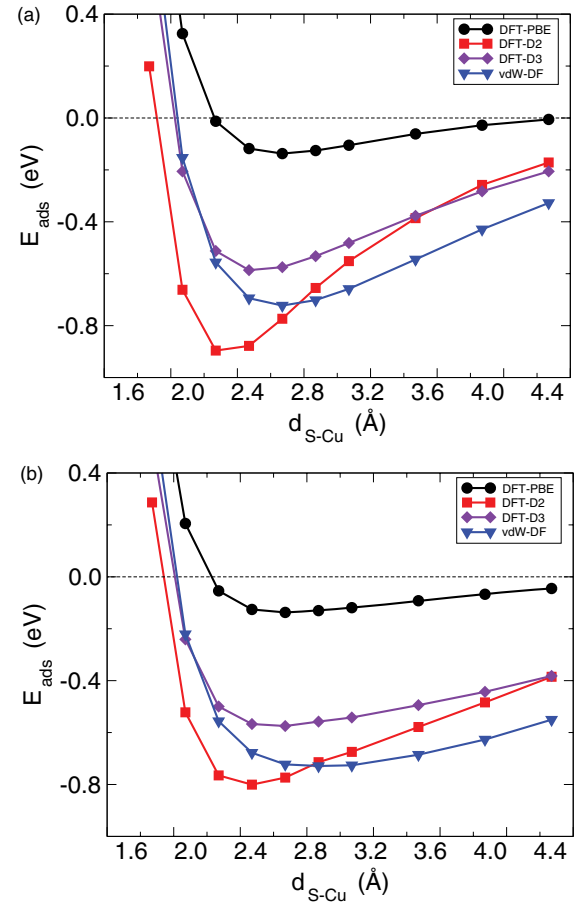

FIG. 4. (Color online) The adsorption energy of a single thiophene molecule adsorbed on the Cu(111) surface as a function of molecule-surface distance calculated with the DFT-PBE, DFT-D2, and DFT-D3 approaches. The vdW-DF calculations have been performed by starting from the DFT-PBE geometry. (a) To calculate the adsorption energy the molecule has been rigidly shifted closer to or farther away from the surface. In (b) the distance between the molecule and the Cu(111) substrate has been fixed while the rest of the molecule was allowed to relax. One can observe that by relaxing the molecular degrees of freedom, the DFT-D2 adsorption curve is less steep in (b) than in (a). On the other hand, these structural relaxations shift the vdW-DF molecule-surface equilibrium distance from 2.67 Å in (a) to 2.87 Å in (b) and also slightly lowers the adsorption energy minimum from −722 meV to −735 meV.

this case the formation of dimers is energetically favored (see Table II).

An important issue investigated in our study is the relevance of the structural relaxations when the vdW energy contribution to the adsorption energy is evaluated for (a) a rigid shift of the DFT-PBE and DFT-D2 molecular equilibrium geometries along a direction O_z perpendicular to the Cu(111) surface and (b) the DFT-PBE molecular geometry is relaxed when displacing the thiophene along O_z by keeping the height of the S atom fixed. Therefore, in case (a) the thiophene molecule in its DFT-PBE ground-state geometry [see Fig. 1(a)] was rigidly shifted closer to or farther away from the surface. On the contrary, in case (b) we have fixed the positions of the S atom and the Cu(111) surface and allowed the rest of the molecule to relax. In this way we obtain a minimum
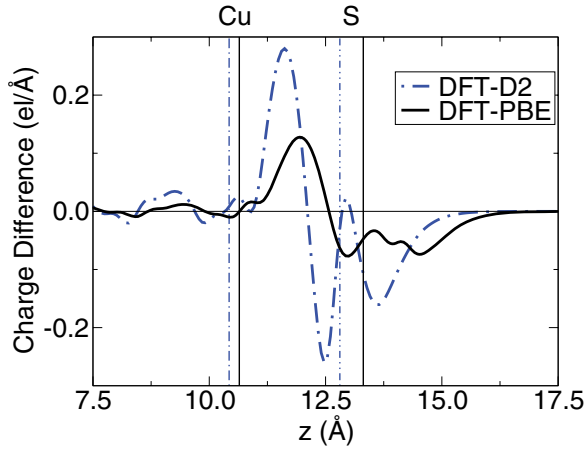
FIG. 5. (Color online) The charge density difference upon adsorption of a single thiophene molecule on the Cu(111) surface integrated over the in-plane directions. The charge transferred from the molecule ($\approx$0.1 and $\approx$0.2 electrons in the case of the DFT-PBE and DFT-D2 calculations, respectively) accumulates between the molecule and the surface (i.e., at the molecule-surface interface). The position along the direction O_z perpendicular to the Cu(111) surface of the Cu surface atom under the thiophene's S one as well as that of the molecule's S atom are also mentioned.

energy configuration under the constraint of the fixed molecule surface distance. Then for each molecule-surface configuration calculated with DFT-PBE for a given adsorbate-substrate distance, we added the semiempirical contribution of the van der Waals energy evaluated with the DFT-D2 and DFT-D3

approaches according to Eq. (3) or we evaluated the adsorption energy employing the vdW-DF functional [see Eq. (4)]. From the adsorption energy vs molecule-surface distance curves shown in Fig. 4, the equilibrium molecule-surface distance as the position of the minimum and the adsorption energy as the depth of the minimum can be obtained. In the case of the DFT-D2 curve one can observe that the molecule-substrate distance of the DFT-D2 equilibrium geometry is reproduced quite well when the molecule is relaxed while an even shorter molecule-surface distance of only 2.2 Å is obtained when the thiophene molecule is rigidly shifted along the O_z direction. However, the DFT-D2 adsorption energy obtained in the (a) and (b) approaches (−0.896 eV and −0.801 eV, respectively) is higher than that obtained when vdW forces were included in the structural relaxation (−1.018 eV; see Table I). The same conclusions can be drawn for the DFT-D3 curves which clearly emphasizes the importance of structural relaxations for a proper description of the molecule-surface system of interest. As regarding the vdW-DF calculations, interestingly, the rigidly shifted DFT-PBE geometries lead to a molecule-surface distance of 2.67 Å and an adsorption energy of $E_{\mathrm{ads}}^{\mathrm{vdW\text{-}DF}} = -722$ meV which are identical to the values reported in Table I for the DFT-PBE geometry. However, the use of the relaxed DFT-PBE geometries [i.e., approach (b)] determines a larger molecule-surface distance of 2.87 Å and a slightly lower adsorption energy of $E_{\mathrm{ads}}^{\mathrm{vdW\text{-}DF}} = -735$ meV.

An adsorption energy of only −137 meV from our DFT-PBE calculations for a single thiophene on Cu(111) would be characteristic for a physisorbed system such as benzene on Au(111)[44,45] where the molecule does not form chemical bonds to the surface. However, in our case the charge
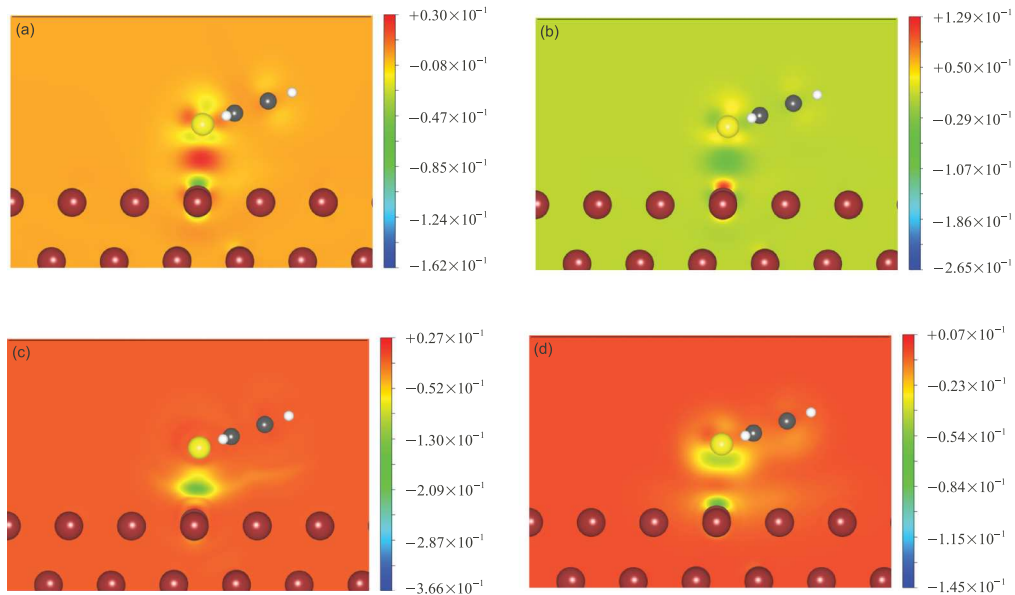

FIG. 6. (Color online) (a) Section of the charge density difference at the center of the S atom upon adsorption of a single thiophene molecule on the Cu(111) surface. The charge transferred from the molecule accumulates between the molecule and the surface. In (b) a section of the LDA correlation binding energy density $\Delta e_c^{\mathrm{LDA}}$, (c) the semilocal correction Δe_c^{SL}, and (d) the nonlocal correction Δe_c^{NL} for the DFT-PBE relaxed geometry are shown. It is important to note that the spatial resemblance between the charge density difference presented in (a) and $\Delta e_c^{\mathrm{LDA}}$ reported in (b) is related to the functional form of the LDA correlation energy functional; i.e., it is local for each charge density point in the real space. On the contrary, a different functional form of the semilocal (in PBE) and the nonlocal (in vdW-DF) correlations lead to a significantly contrasting spatial behavior of the Δe_c^{SL} and Δe_c^{NL}, respectively. This figure has been generated using VESTA (Ref. 43).
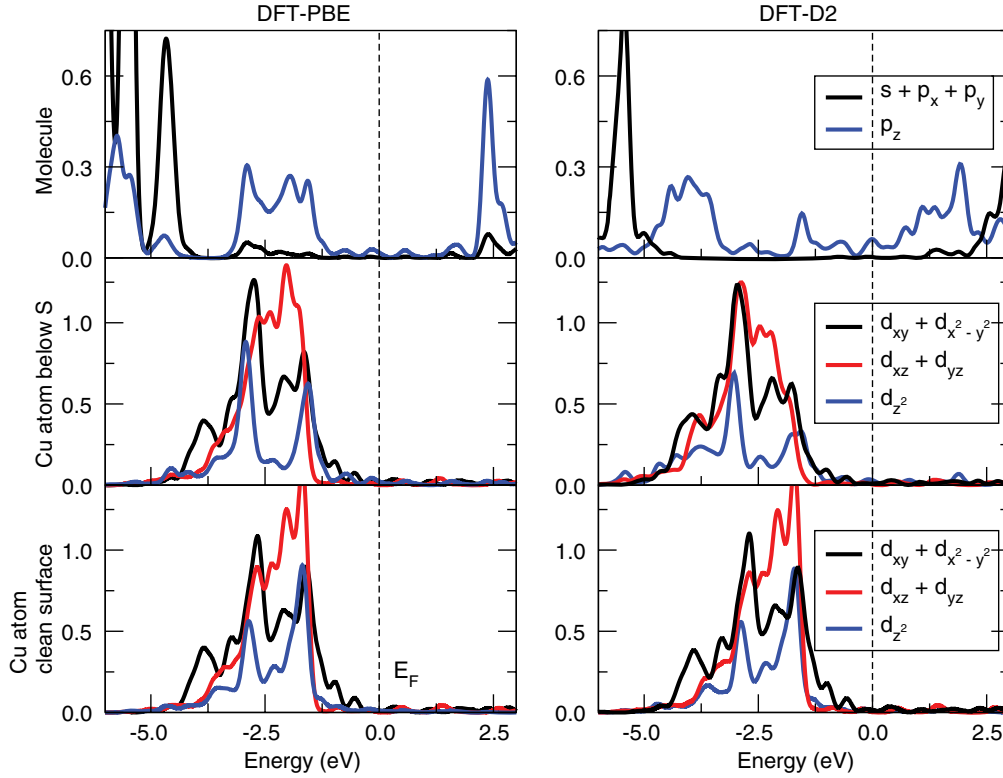
FIG. 7. (Color online) The density of states projected on specific atomic orbitals for a single thiophene molecule adsorbed on Cu(111) for the relaxed molecule-surface geometry obtained without (DFT-PBE) and by including vdW interactions (DFT-D2). The projected density of states (PDOS) has been broadened by a 0.1 eV Gaussian. A stronger hybridization between the molecular electronic states and those of the Cu(111) substrate observed for the DFT-D2 calculations is related to a flat thiophene geometry [see Fig. 5(c)] which enhances the interaction of the molecular π electrons with the Cu atomic states of appropriate symmetry. Note that the PDOS obtained for a Cu atom of the clean surface is the same in both DFT-PBE and DFT-D2 calculations; i.e., it is not affected by the vdW interactions. For convenience, the Fermi level E_F was set to zero.

density difference plots suggest a weak chemisorption bonding process. As depicted in Fig. 5, upon adsorption of thiophene on the Cu(111) surface a small amount of charge (≈ 0.1 and ≈ 0.2 electrons for DFT-PBE and DFT-D2 calculations, respectively) is transferred from the molecule to interface and accumulates between the molecule and surface. Besides this, as shown in Fig. 6(a), at the molecular site a charge rearrangement process also takes place which implies that the bonding of a single thiophene to the Cu(111) surface involves both the π-electron system and the sulfur lone-pair electrons.

In consequence, it is important to investigate the origin of the difference between $E_{ads}^{DFT-PBE}$ and E_{ads}^{vdW-DF} evaluated for the *same* ground-state molecule-surface adsorption geometry and its corresponding charge density. Since we used the same exchange functional for both calculations, the difference between these two adsorption energies can be expressed as $E_{ads}^{DFT-PBE} - E_{ads}^{vdW-DF} = \Delta E_c^{SL} - \Delta E_c^{NL}$, where ΔE_c^{SL} and ΔE_c^{NL} are the semilocal and the nonlocal correlation binding energy contributions to $E_{ads}^{DFT-PBE}$ and E_{ads}^{vdW-DF}, respectively. The real-space correlation binding energy density Δe_c^{PBE}, which is the difference between the correlation energy density of the molecule-surface system and the sum of the free molecule and the clean surface evaluated for the relaxed DFT-PBE thiophene-Cu(111) geometry, is depicted in Figs. 6(b)–6(d). One can observe that the shape of the LDA correlation binding

energy density Δe_c^{LDA} corresponds well to the charge density difference Δn due to the functional form of LDA. In particular, a significant contribution to Δe_c^{LDA} comes from the bonding region between the surface Cu atom and the S one above it [see Fig. 6(b)]. The semilocal correlation binding energy density Δe_c^{SL} corresponds to the semilocal correction to the LDA one. It is spatially confined to areas where the LDA correlation binding energy density also has a contribution [see Fig. 6(c)]. This behavior is due to the fact that the semilocal corrections require only the information about nearest-neighbor charge density points through the charge density gradient. In contrast, the nonlocal correlation functional connects each charge density point with all other charge density points in the real space and thus the corresponding nonlocal correlation binding energy density Δe_c^{NL} can have contributions from domains which are not relevant for the semilocal one Δe_c^{SL}. Indeed, as clearly shown in Fig. 6(d), the nonlocal correlation binding energy is spatially localized mainly around the sulfur atom and the Cu atom underneath while the semilocal correlation binding energy is mainly localized in a region between these atoms where the weak chemical bond is formed [see Fig. 6(c)]. In the Supplemental Material[46] we attach movies that illustrate more clearly this striking difference. It is also important to note that a similar physical picture has been obtained when the vdW-DF method was applied to DFT-D2 and DFT-D3 relaxed geometries.

C. Electronic structure

We have already discussed in Sec. III A that for a single thiophene molecule the DFT-PBE geometry is closer to the experimental one than the DFT-D2 geometry. Nevertheless, from a theoretical point of view, it is important to investigate the flat DFT-D2 adsorption geometry as a limiting theoretical case even if so far no experimental evidence for such flat geometry is available. Since the molecule-metal distance is different for the tilted DFT-PBE and flat DFT-D2 adsorption geometries, it may be interesting to analyze the difference between their electronic structure. Therefore, in Fig. 7 we report the projected density of states (PDOS) for the single thiophene molecule adsorbed on Cu(111) obtained for the DFT-PBE and DFT-D2 adsorption configurations. The upper panel shows the projections on the s and p states of the C, S, and H atoms which in the case of a gas-phase thiophene molecule would correspond to σ- and π-type molecular orbitals. The PDOS obtained for the DFT-PBE calculations reveals that the interaction between the p_z atomic-type orbitals of the molecule with the d states of the metal leads to the formation of hybrid molecule-surface interface states in an energy range between -3 eV and -1.25 eV. When including the vdW interactions, the thiophene molecule comes closer to surface leading to a stronger molecule-surface interaction and, therefore, most of these interface states are shifted to lower energies. In addition, the sharp peak present at 2.1 eV above Fermi level in the DFT-PBE PDOS diagram is broadened and shifted to lower energies when including the vdW interactions. The middle panels of Fig. 7 present the PDOS of the Cu atom below the S one while the lower panels show the PDOS of an Cu atom of the clean surface. One can observe that the shape of the in-plane d states (d_{xy} and $d_{x^2-y^2}$) are practically not affected by the adsorption of thiophene onto the Cu surface, while the shape of the out-of-plane d orbitals (d_{xz}, d_{yz}, and d_{z^2}) is changed due to the strong molecule-metal hybridization. Moreover, the out-of-plane d orbitals are pushed to lower energies in the case of the DFT-D2 geometry as compared to the DFT-PBE one. We also note that similar PDOS features are present in the case of thiophene dimers or 4-thiophene molecules adsorption on the Cu surface.

The differences in the electronic structures of the two DFT-PBE and DFT-D2 geometries can be easily observed in the simulated constant current images (see Fig. 8) within the Tersoff-Hamann (TH) model[47] for several bias voltages. These images are obtained by plotting isosurfaces of the energy integrated charge density from the Fermi level up to a given bias voltage. These isosurfaces correspond to surfaces of constant current within TH model. The STM images obtained with the relaxed DFT-PBE geometry do not vary much with the bias voltage. For negative bias voltages (corresponding to the occupied molecule-surface states) they show a round-shaped feature which is slightly more rectangular for positive bias voltages (corresponding to the unoccupied molecule-surface states). Due to a tilted DFT-PBE adsorption geometry, a slight asymmetry of the simulated STM images can be observed as a brighter upper part of these images. In contrast to the DFT-PBE case, the simulated STM images for the DFT-D2 relaxed geometry show a clear pentagonal structure for negative bias
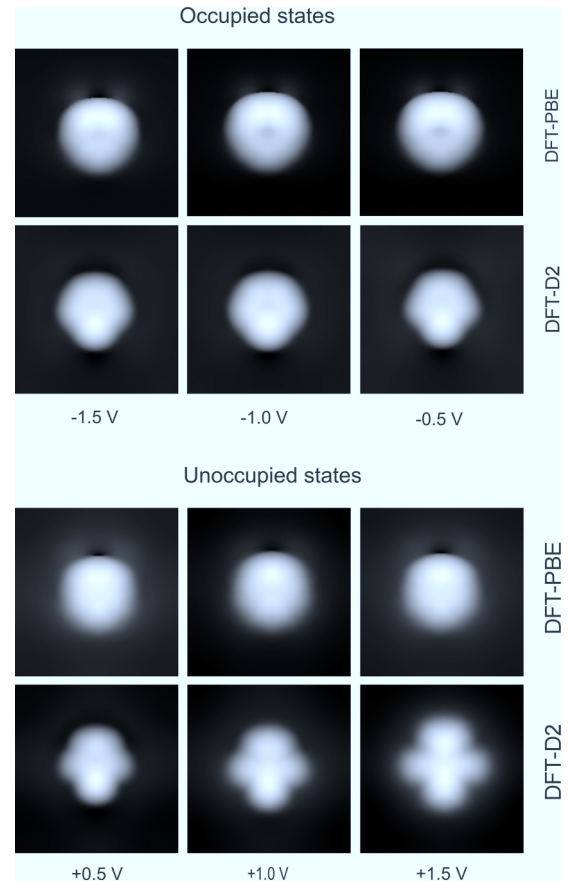

FIG. 8. Simulated STM images within the Tersoff-Hamann model in constant current mode compared for the DFT-PBE and DFT-D2 relaxed geometries for several bias voltages. Within this model the surfaces of constant charge integrated from the Fermi level to the bias voltage, shown in this figure, are proportional to the tunneling current.

voltages. For positive bias voltages, this contrast is enhanced since the STM images have a crosslike shape. Overall, the topographic differences between the STM images at the same bias voltage obtained for the tilted DFT-PBE and flat DFT-D2 geometries are due to a stronger molecule-surface hybridization in the DFT-D2 case. We suggest that the clear features present in the simulated STM images for the flat DFT-D2 geometry (as a limit case for a stronger molecule-surface interaction than that predicted for a single molecule) at positive bias voltages could be easily identified in an STM experiment.

IV. CONCLUSIONS

To summarize, in this *ab initio* study we have investigated the adsorption of thiophene, 4-thiophene, and their dimers on the Cu(111) surface. The relevance of the London dispersion effects on the molecule-surface adsorption geometry and the corresponding binding energy was evaluated by means of two semiempirical methods (DFT-D2 and DFT-D3, respectively) as well as by employing a nonlocal correlation energy functional (vdW-DF) developed from first principles. From the geometrical point of view, in the case of a single thiophene on the Cu(111) substrate the DFT-PBE relaxed geometry is

quite close to the experimental one with a tilt angle of $18°$ and a molecule-surface distance of 2.67 Å while the DFT-D2 calculations predict a flat adsorption geometry. It is interesting to note that the tilt angle of the DFT-D3 relaxed geometry is between the DFT-PBE and DFT-D2 values while its thiophene-Cu(111) distance is identical to the DFT-PBE one. From the energetic point of view, the DFT-PBE calculations predict that a single thiophene molecule on Cu(111) is physisorbed with an adsorption energy of $−0.137$ eV while the DFT-D2 approach significantly overestimates it. Importantly, the adsorption energy calculated with the DFT-D3 method is quite close to the experimental value ($−0.59$ eV). However, for the DFT-PBE relaxed geometry, the use of the nonlocal correlation energy functional vdW-DF changes the strength of the interaction between a single thiophene molecule with the Cu(111) surface from a value characteristic to a physisorption bonding mechanism to one corresponding to a weak chemisorption. This change is related to a different behavior of the nonlocal (vdW-DF) versus semilocal (PBE) correlations as clearly illustrated by the plots of the adsorption binding energy density in the real space. We have also studied the electronic structure of a single thiophene molecule adsorbed on Cu(111) and the predicted STM images for the DFT-PBE and DFT-D2 geometries show a clear difference which could be easily observed in an STM experiment. As regarding the 4-thiophene on Cu(111), both DFT-PBE and DFT-D2 methods predict that a single 4-thiophene will adsorb with the molecular long axis aligned along the $\langle 110 \rangle$ surface direction instead of the $\langle 11\text{-}2 \rangle$ one as suggested by recent STM experiments. Finally, the DFT-PBE as well as DFT-D2 calculations show that the adsorption of thiophene and 4-thiophene dimers are energetically favorable with respect to that of single molecules.

APPENDIX: JuNoLo UPDATE

The nonlocal correlation energy E_c^NL and its density $e_\text{c}^\text{NL}(\mathbf{r})$ given in Eqs. (5) and (6) are calculated by using the JuNoLo code.[41] In the initial version of this code, these quantities are calculated by replacing the double integral in Eq. (5) by a double sum evaluated directly in real space. In this study, we have updated the JuNoLo code with the scheme proposed by Román-Pérez and Soler.[40] This method allows a very efficient integration of Eq. (5) by interpolating the kernel $\phi(\mathbf{r},\mathbf{r}')$ in order to bring it to a separable form. Then by using a Fourier transform the double spatial integral is reduced to a single one. Within this formalism Eq. (5) takes the form

$$E_\text{c}^\text{NL} = \frac{1}{2} \sum_{\alpha,\beta} \int \Theta_\alpha^*(\mathbf{k})\Theta_\beta(\mathbf{k})\phi_{\alpha\beta}(k)\, d^3\mathbf{k}, \qquad \text{(A1)}$$

where $\Theta_\alpha(\mathbf{k})$ is the Fourier transform of the function $\Theta_\alpha(\mathbf{r}) = n(\mathbf{r})p_\alpha(q)$ which is charge density $n(\mathbf{r})$ times an expansion polynomial $p_\alpha(q)$. The variable $q = q(n(\mathbf{r}),\nabla n(\mathbf{r}))$ is a function of the charge density $n(\mathbf{r})$ and its gradient $\nabla n(\mathbf{r})$ at a given position $\mathbf{r}$ and the sum over α,β runs over all interpolation points N_α.

In this method, one can also express the nonlocal correlation energy density $e_\text{c}^\text{NL}(\mathbf{r})$ defined in Eq. (6) as

$$e_\text{c}^\text{NL}(\mathbf{r}) = \frac{1}{2} \sum_\alpha \Theta_\alpha(\mathbf{r})u_\alpha(\mathbf{r}), \qquad \text{(A2)}$$

where $u_\alpha(\mathbf{r}) = \sum_\beta \int \Theta_\beta(\mathbf{r}')\phi_{\alpha\beta}(\mathbf{r} - \mathbf{r}')d^3\mathbf{r}'$ is the convolution of $\Theta_\alpha(\mathbf{r})$ with the kernel $\phi_{\alpha\beta}(\mathbf{r} - \mathbf{r}')$ which has been defined in the original paper[40] to calculate the nonlocal contribution to the potential. Our updated version of the JuNoLo code is now able to calculate not only the nonlocal correlation energy contribution to the total energy but also the nonlocal correlation potential taking the speed advantage of the Pérez-Soler scheme.

[*]n.atodiresei@fz-juelich.de

[1]H. Song, M. A. Reed, and T. Lee, Adv. Mater. **23**, 1583 (2011).

[2]A. Aviram and M. A. Ratner, Chem. Phys. Lett. **29**, 277 (1974).

[3]M. Elbing, R. Ochs, M. Koentopp, M. Fischer, C. von Hänisch, F. Weigend, F. Evers, H. B. Weber, and M. Mayor, Proc. Natl. Acad. Sci. USA **102**, 8815 (2005).

[4]I. Díez-Pérez, J. Hihath, Y. Lee, L. Yu, L. Adamska, M. A. Kozhushner, I. I. Oleynik, and N. Tao, Nat. Chem. **1**, 635 (2009).

[5]V. C. Sundar, J. Zaumseil, V. Podzorov, E. Menard, R. L. Willett, T. Someya, M. E. Gershenson, and J. A. Rogers, Science **303**, 1644 (2004).

[6]A. S. Blum, J. G. Kushmerick, D. P. Long, C. H. Patterson, J. C. Yang, J. C. Henderson, Y. Yao, J. M. Tour, R. Shashidhar, and B. R. Ratna, Nat. Mater. **4**, 167 (2005).

[7]S. Y. Quek, M. Kamenetska, M. L. Steigerwald, H. J. Choi, S. G. Louie, M. S. Hybertsen, J. B. Neaton, and L. Venkataraman, Nat. Nanotechnol. **4**, 230 (2009).

[8]J. E. Green, J. W. Choi, A. Boukai, Y. Bunimovich, E. Johnston-Halperin, E. DeIonno, Y. Luo, B. A. Sheriff, K. Xu, Y. S. Shin, H.-R. Tseng, J. F. Stoddart, and J. R. Heath, Nature (London) **445**, 414 (2007).

[9]K. Moth-Poulsen and T. Bjørnholm, Nat. Nanotechnol. **4**, 551 (2009).

[10]S. Karthäuser, J. Phys.: Condens. Matter **23**, 013001 (2011).

[11]E. C. P. Smits, S. G. J. Mathijssen, P. A. van Hal, S. Setayesh, T. C. T. Geuns, K. A. H. A. Mutsaers, E. Cantatore, H. J. Wondergem, O. Werzer, R. Resel, M. Kemerink, S. Kirchmeyer, A. M.

Muzafarov, S. A. Ponomarenko, B. de Boer, P. W. M. Blom, and D. M. de Leeuw, Nature (London) **455**, 956 (2008).

[12] J. Repp, P. Liljeroth, and G. Meyer, Nat. Phys. **6**, 975 (2010).

[13] P. Milligan, J. McNamarra, B. Murphy, B. C. C. Cowie, D. Lennon, and M. Kadodwala, Surf. Sci. **412-413**, 166 (1998).

[14] P. K. Milligan, B. Murphy, D. Lennon, B. C. C. Cowie, and M. Kadodwala, J. Phys. Chem. C **105**, 140 (2001).

[15] A. Imanishi, T. Yokoyama, Y. Kitajima, and T. Ohta, Bull. Chem. Soc. Jpn. **71**, 831 (1998).

[16] G. B. D. Rousseau, N. Bovet, S. M. Johnston, D. Lennon, V. Dhanak, and M. Kadodwala, Surf. Sci. **511**, 190 (2002).

[17] M. Kiguchi, G. Yoshikawa, and K. Saiki, J. Appl. Phys. **94**, 4866 (2003).

[18] T. Kakudate, S. Tsukamoto, M. Nakaya, and T. Nakayama, Surf. Sci. **605**, 1021 (2011).

[19] H. Orita and N. Itoh, Surf. Sci. **550**, 177 (2004).

[20] C. Morin, A. Eichler, R. Hirschl, P. Sautet, and J. Hafner, Surf. Sci. **540**, 474 (2003).

[21] P. Sony, P. Puschnig, D. Nabok, and C. Ambrosch-Draxl, Phys. Rev. Lett. **99**, 176401 (2007).

[22] K. Tonigold and A. Gross, J. Chem. Phys. **132**, 224701 (2010).

[23] F. Buonocore and A. di Matteo, Theoretical Chemistry Accounts: Theory, Computation, and Modeling (Theoretica Chimica Acta) **124**, 217 (2009).

[24] J. Zhou, Y. X. Yang, P. Liu, N. Camillone, III, and M. G. White, J. Phys. Chem. C **114**, 13670 (2010).

[25] G. Kresse and J. Furthmüller, Phys. Rev. B **54**, 11169 (1996).

[26] G. Kresse and J. Furthmüller, Comput. Mater. Sci. **6**, 15 (1996).

[27] G. Kresse and J. Hafner, Phys. Rev. B **47**, 558 (1993).

[28] G. Kresse and J. Hafner, Phys. Rev. B **49**, 14251 (1994).

[29] J. P. Perdew, K. Burke, and M. Ernzerhof, Phys. Rev. Lett. **77**, 3865 (1996).

[30] P. E. Blöchl, Phys. Rev. B **50**, 17953 (1994).

[31] D. C. Langreth, B. I. Lundqvist, S. D. Chakarova-Käck, V. R. Cooper, M. Dion, P. Hyldgaard, A. Kelkkanen, J. Kleis, L. Kong, S. Li, P. G. Moses, E. Murray, A. Puzder, H. Rydberg, E. Schröder, and T. Thonhauser, J. Phys.: Condens. Matter **21**, 084203 (2009).

[32] F. London, Z. Phys. **63**, 245 (1930).

[33] S. Grimme, J. Comput. Chem. **27**, 1787 (2006).

[34] N. Atodiresei, V. Caciuc, P. Lazić, and S. Blügel, Phys. Rev. Lett. **102**, 136809 (2009).

[35] K. Toyoda, I. Hamada, K. Lee, S. Yanagisawa, and Y. Morikawa, J. Chem. Phys. **132**, 134703 (2010).

[36] K. Toyoda, I. Hamada, K. Lee, S. Yanagisawa, and Y. Morikawa, J. Phys. Chem. C **115**, 5767 (2011).

[37] G. Mercurio, E. R. McNellis, I. Martin, S. Hagen, F. Leyssner, S. Soubatch, J. Meyer, M. Wolf, P. Tegeder, F. S. Tautz, and K. Reuter, Phys. Rev. Lett. **104**, 036102 (2010).

[38] S. Grimme, J. Antony, S. Ehrlich, and H. Krieg, J. Chem. Phys. **132**, 154104 (2010).

[39] M. Dion, H. Rydberg, E. Schröder, D. C. Langreth, and B. I. Lundqvist, Phys. Rev. Lett. **92**, 246401 (2004).

[40] G. Román-Pérez and J. M. Soler, Phys. Rev. Lett. **103**, 096102 (2009).

[41] P. Lazic, N. Atodiresei, M. Alaei, V. Caciuc, S. Blügel, and R. Brako, Comput. Phys. Commun. **181**, 371 (2010).

[42] M. May, S. Gonzalez, and F. Illas, Surf. Sci. **602**, 906 (2008).

[43] K. Momma and F. Izumi, J. Appl. Crystallogr. **44**, 1272 (2011).

[44] E. R. McNellis, J. Meyer, and K. Reuter, Phys. Rev. B **80**, 205414 (2009).

[45] J. Wellendorff, A. Kelkkanen, J. Mortensen, B. Lundqvist, and T. Bligaard, Topics Catal. **53**, 378 (2010).

[46] See Supplemental Material at http://link.aps.org/supplemental/10.1103/PhysRevB.86.085439 for movies.

[47] J. Tersoff and D. R. Hamann, Phys. Rev. Lett. **50**, 1998 (1983).